[Water Resources Research]

Supporting Information for

Diffuse Groundwater Discharge Dominates Terrestrial Dissolved Inorganic Carbon Export and CO_2 Evasion From a Semiarid Headwater Stream

Chuan Wang[1], Yueqing Xie[1,2,*], Shaoda Liu[3], James L. McCallum[4], Qing Li[5], and Jichun Wu[1,*]

[1]Ministry of Education Key Laboratory of Surficial Geochemistry, School of Earth Sciences and Engineering, Nanjing University, Nanjing, China

[2]National Centre for Groundwater Research and Training, College of Science and Engineering, Flinders University, Adelaide, South Australia, Australia

[3]Yale School of Forestry and Environmental Studies, Yale University, New Haven, Connecticut, USA

[4]School of Earth Sciences, University of Western Australia, Perth, Western Australia, Australia

[5]State Key Laboratory of Marine Environment Science, College of Ocean & Earth Sciences, Xiamen University, Xiamen, China

[*]Corresponding author: Yueqing Xie (yxie@nju.edu.cn)

Jichun Wu (jcwu@nju.edu.cn)

Contents of this file

Additional Supporting Information (Files uploaded separately)

Tables S7. Data set of Hailiutu River

Introduction

Text S1 demonstrates the calculation of pCO_2 and DIC in our study. Text S2 shows how we derived the empirical stream CO_2 evasion rate. Figure S1 shows the calibrated water and mass balance parameters derived from MCMC modeling. Figure S2 depicts the relationship between carbonate buffering transformation and net internal CO_2 production. Table S1-S3 are the measured data and parameters for water and carbon balance calculation. Table S4 shows the initial parameters used for PHREEQC simulation. Table S5 is the measured carbon isotopic data. Table S6 is the comparison of different headwater stream CO_2 evasion rates. All measurements were obtained between 9 and 14 May 2019 (dry season), and according to the methods described in the manuscript. Table S7 is all the related data used in this study, and uploaded separately as excel file.

Text S1. pCO_2 and DIC calculation

Dissolved inorganic carbon (DIC) is defined as the sum of CO_2^* (i.e., $CO_{2(aq)}$ + H_2CO_3), HCO_3^- and CO_3^{2-}. The relative proportion of the three inorganic carbon species (partition coefficient) depends on pH and temperature in water

$$\alpha_0 = \left(1 + \frac{K_1}{\left[H^+\right]} + \frac{K_1 K_2}{\left[H^+\right]^2}\right)^{-1} \quad \text{(S1)}$$

$$\alpha_1 = \left(1 + \frac{\left[H^+\right]}{K_1} + \frac{K_2}{\left[H^+\right]}\right)^{-1} \quad \text{(S2)}$$

$$\alpha_2 = \left(1 + \frac{\left[H^+\right]^2}{K_1 K_2} + \frac{\left[H^+\right]}{K_2}\right)^{-1} \quad \text{(S3)}$$

where α_0, α_1, and α_2 are the partition coefficient of CO_2^*, HCO_3^- and CO_3^{2-}, respectively. $\left[H^+\right]$ is the activity of H^+ (mol/L), which equals 10^{-pH}. K_1 and K_2 are the temperature-dependent first and second dissociation constant for the dissociation of H_2CO_3, respectively. K_1 and K_2 are determined according to empirical equations from Clark and Fritz (1997)

$$-\log_{10}\left(K_1\right) = 1.1 \times 10^{-4} T^2 - 0.012T + 6.58 \quad \text{(S4)}$$

$$-\log_{10}\left(K_2\right) = 9 \times 10^{-5} T^2 - 0.0137T + 10.62 \quad \text{(S5)}$$

where T is the temperature in water (°C).

Alkalinity is defined as

$$Alkalinity = \left[HCO_3^-\right] + 2\left[CO_3^{2-}\right] + \left[OH^-\right] - \left[H^+\right] \\ = \alpha_1 DIC + 2\alpha_2 DIC + \left[OH^-\right] - \left[H^+\right] \quad \text{(S6)}$$

Rearranging Equation (S6) leads to the expression of DIC

$$DIC = \frac{1}{\alpha_1 + 2\alpha_2}\left(Alkalinity + \left[H^+\right] - \left[OH^-\right]\right) \quad \text{(S7)}$$

when pH is 5~9 and $Alkalinity$ > 1 meq/L, $\left[H^+\right] - \left[OH^-\right]$ can be neglected and the expression of DIC can be simplified into

$$DIC = \frac{1}{\alpha_1 + 2\alpha_2} Alkalinity \quad \text{(S8)}$$

where the unit of $Alkalinity$ is meq/L, α_1 and α_2 can be derived from Equation (S2) and (S3), respectively, and the unit of DIC is mmol/L.

According to Plummer and Busenberg (1982), the partial pressure of CO_2 (pCO_2, atm) can be calculated by (all the variables are in mol/L)

$$pCO_2 = \frac{HCO_3^- \times H^+}{K_H \times K_1} \quad \text{(S9)}$$

where HCO_3^- is the activity of bicarbonate and can be determined by multiplying the DIC (mol/L) and the partition coefficient α_1, H^+ equals 10^{-pH}, and K_1 can be derived through Equation (S4). K_H is the Henry's law constant (mol/L/atm), and can be derived from Clark and Fritz (1997)

$$-\log_{10}\left(K_H\right) = -7 \times 10^{-5} T^2 + 0.016T + 1.11 \quad \text{(S10)}$$

where T is the temperature in water (°C).

Text S2. Empirical stream CO_2 evasion model

We utilized Equation (7) in Raymond et al. (2012) to estimate the normalized K_{CO_2} with a Schmidt number of 600 (k_{600})

$$k_{600} = 4725 \times (VS)^{0.86} \times Q^{-0.14} \times D^{0.66} \tag{S11}$$

where V , S , Q , and D are the stream velocity (m/s), slope (dimensionless), stream flow rate (m^3/s), and stream depth (m). S is derived from Digital Elevation Model in our study area, and the other variables (V , Q , and D) are field measured values.

Empirical K_{CO_2} can be calculated by

$$K_{CO_2} = k_{600} \times \left(\frac{Sc_{CO_2}}{600} \right)^{-0.5} \tag{S12}$$

where Sc_{CO_2} is the Schmidt number of the field measured stream temperature (°C) and derived from Raymond et al. (2012)

$$Sc_{CO_2} = 1742 - 91.24T + 2.208T^2 - 0.0219T^3 \tag{S13}$$

The stream CO_2 evasion rate ($F_{air}^{CO_2}$, g C m^{-2} d^{-1}) of the empirical model was calculated by

$$F_{air}^{CO_2} = \left(pCO_{2\ aq} - pCO_{2\ air} \right) \times K_H \times K_{CO_2} \times 12 \div 1000 \tag{S14}$$

where $pCO_{2\,aq}$ and $pCO_{2\,air}$ are the CO_2 partial pressure in the stream and the air (μatm), respectively. We assumed that the atmospheric pCO_2 was 390 μatm. K_H and K_{CO_2} are the temperature-dependent Henry's Law constant (mol/L/atm) derived from Equation (S10) and the CO_2 gas transfer velocity (m/d) derived from Equation (S12).

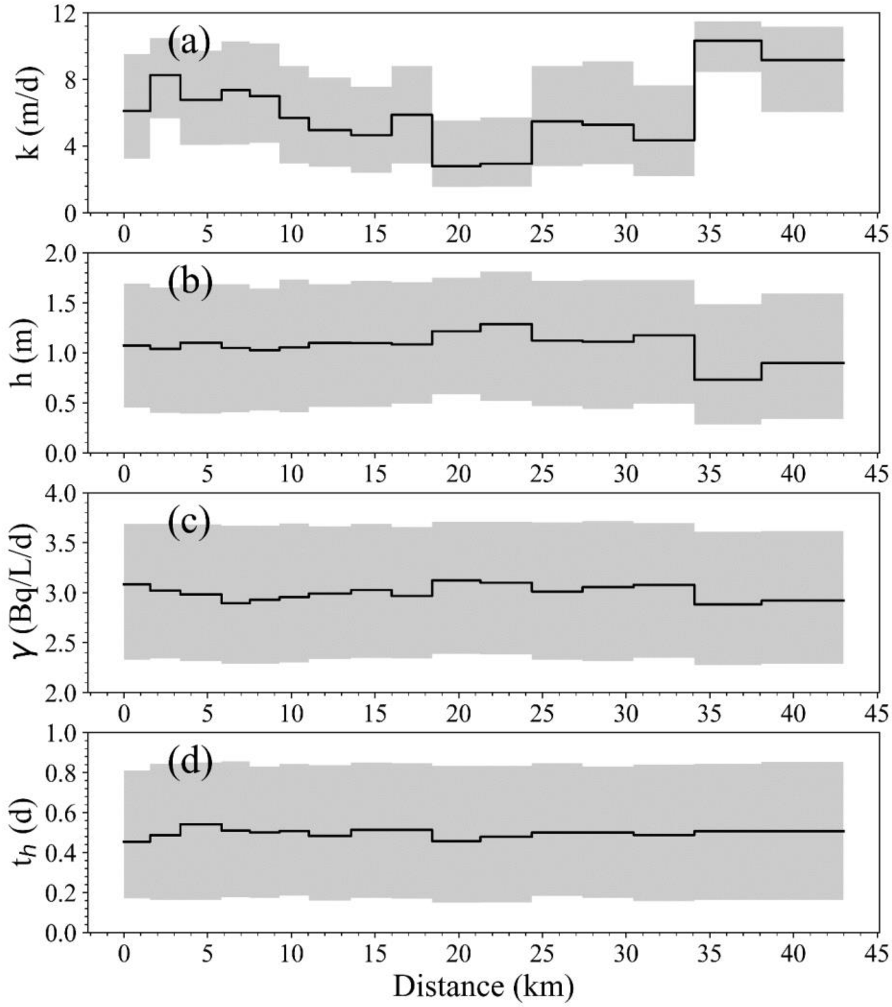

Figure S1. Longitudinal spatial variability of the optimal model parameters and corresponding uncertainty bounds (16^{th}-84^{th} percentiles) including (a) ^{222}Rn gas transfer velocity (*k*), (b) hyporheic zone thickness (*h*), (c) ^{222}Rn production rate in the hyporheic zone (γ), and (d) hyporheic zone residence time (t_h) derived from the evolutionary Markov chain Monte-Carlo simulation.

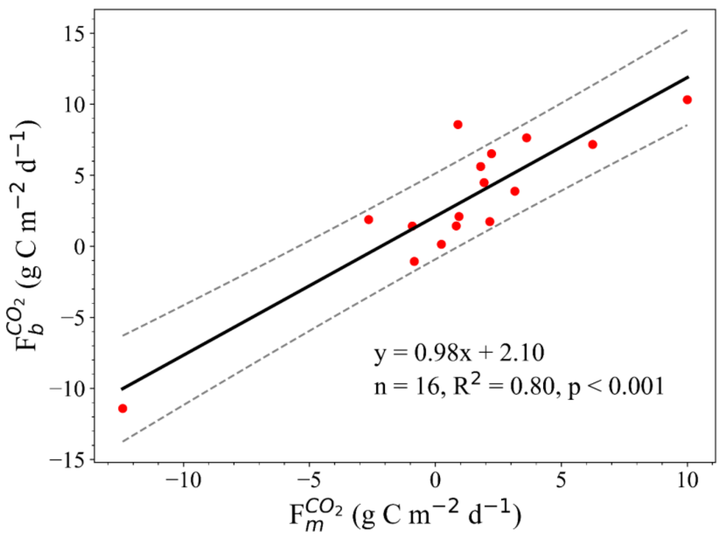

Figure S2. The positive relationship between carbonate buffering transformation ($F_b^{CO_2}$) and net internal CO_2 production ($F_m^{CO_2}$). The black line is the linear regression result, while the grey dashed lines are the 10% and 90% confidence intervals.

	Distance	Flow rate *Q*	Width *w*	Depth[a] *d*	Velocity[b] *v*	Stream		Groundwater	
-	km	m^3/s	m	m	m/s	EC(μS/cm)	^{222}Rn(Bq/L)	EC(μS/cm)	^{222}Rn(Bq/L)
Hailiutu-01	0	0.283	6.3	0.19	0.234	994	1.080	659	4.830
Hailiutu-02	1.57	0.343	4.1	0.24	0.347	887	1.080	640	5.340
Hailiutu-03	3.37	0.440	4.7	0.49	0.190	726	1.150	396	6.442
Hailiutu-04	5.83	0.547	4.4	0.42	0.294	699	1.119	648	4.922
Hailiutu-05	7.52	0.596	3.8	0.33	0.477	619	1.049	396	5.337
Hailiutu-06	9.30	0.713	5.2	0.41	0.338	576	0.837	609	5.077
Hailiutu-07	11.05	0.693	8.2	0.15	0.578	631	0.832	376	5.470
Hailiutu-08	13.57	0.793	9.6	0.11	0.735	581	0.837	375	4.797
Hailiutu-09	15.99	1.394	8.0	0.19	0.930	686	0.904	338	5.707
Hailiutu-10	18.41	0.949	5.9	0.22	0.727	612	0.944	558	5.707
Hailiutu-11	21.29	1.191	7.9	0.21	0.705	563	1.020	679	4.020
Hailiutu-12	24.37	0.845	6.2	0.17	0.808	516	0.978	420	6.636
Hailiutu-13	27.39	0.898	5.0	0.19	0.956	491	1.046	517	4.070
Hailiutu-14	30.44	1.116	11.0	0.13	0.786	485	0.731	488	4.350
Hailiutu-15	34.08	1.085	5.3	0.21	0.958	456	0.800	628	4.755
Hailiutu-16	38.09	1.824	6.8	0.31	0.869	457	0.383	241	4.482
Hailiutu-17	42.98	2.093	5.4	0.34	1.156	472	0.322	674	4.447

Table S1. Field measured values for reach-scale water and mass balance modeling. [a] *d* equals the cross-section area divided by the stream width. [b] *v* equals the stream flow rate divided by the cross-section area. The Bulang River (Q, EC and ^{222}Rn activity are 0.076 m^3/s, 433 μS/cm and 0.767 Bq/L, respectively) flows into the Hailiutu River at the distance of 14 km. Three irrigation diversion points exist between Hailiutu-01~Hailiutu-02, Hailiutu-04~Hailiutu-05, and Hailiutu-09~Hailiutu-10, and their outgoing fluxes are 0.071, 0.116, and 0.557 m^3/s, respectively.

Type	Symbol	Description	Values
Fixed[a]	E	Evaporation rate	0.005 m/d
	θ	Hyporheic zone porosity	0.38
	λ	Radioactive constant of ^{222}Rn	0.18 d^{-1}
	w	Stream width	Measured values
	d	Stream depth	Measured values
	C_{gw}	Groundwater ^{222}Rn activity (or EC)	Measured values
	C_{Tri}	Tributary ^{222}Rn activity (or EC)	Measured values
	Q_0	Incoming stream flow rate	0.283 m^3/s
	C_0	Incoming stream ^{222}Rn activity (or EC)	1.08 Bq/L (or 994 µS/cm)
Calibrated[b]	I	Groundwater discharge	0-10 m^2/d
	k	^{222}Rn gas transfer velocity	1-12 m/d
	h	Hyporheic zone thickness	0.1-2 m
	γ	^{222}Rn production rate in hyporheic zone	2-4 Bq/L/d
	t_h	Hyporheic zone residence time	0.01-1 d
Modeled	Q	Stream flow rate	-
	C	Stream ^{222}Rn activity (or EC)	-

Table S2. Model parameters for reach-scale water and mass balance modeling. [a] E usually varies in 10^{-3}-10^{-2} m/d and is negligible (Cook et al., 2003; Cook et al., 2006). θ was taken from (Ma et al., 2017). λ is a constant value of 0.18 d^{-1}. For a given stream reach, w, d, C_{gw}, and C_{Tri} are the mean values between two measurement points. [b] The calibrated parameter ranges were chosen according to literature review (Cook, 2013; Cook et al., 2006; McCallum et al., 2012; Raymond et al., 2012; Xie et al., 2016)

Measured	Temperature	pH	DO	Alkalinity	DIC	DOC	pCO_2	Ca^{2+}	Mg^{2+}	IAP/K(calcite)
	℃	-	mg/L	meq/L	mg/L	mg/L	μatm	mg/L	mg/L	-
Stream										
Hailiutu-01	14.8	8.48	10.30	5.14	61.55	5.71	954	76.50	34.38	15.49
Hailiutu-02	17.7	8.76	9.40	4.76	56.12	5.86	470	75.13	32.15	27.54
Hailiutu-03	12.1	8.36	8.71	4.74	57.13	5.18	1131	65.59	28.53	9.12
Hailiutu-04	13.3	8.49	9.17	3.82	45.75	4.91	681	67.33	27.33	10.47
Hailiutu-05	15.6	8.63	9.34	4.20	49.92	4.75	552	63.52	24.50	15.85
Hailiutu-06	15.9	8.65	9.15	3.95	46.90	5.25	497	60.84	23.12	15.14
Hailiutu-07	12.2	8.38	9.48	3.70	44.56	4.97	843	59.54	19.66	7.24
Hailiutu-08	21.5	8.50	7.67	3.68	43.90	4.86	706	57.13	18.10	11.75
Hailiutu-09	15.3	8.52	8.25	3.60	43.02	4.93	611	60.36	19.62	10.47
Hailiutu-10	9.7	8.49	9.74	3.78	45.35	8.08	648	58.74	19.16	8.51
Hailiutu-11	13.1	8.46	8.72	3.90	46.78	5.49	744	57.49	18.10	8.91
Hailiutu-12	17.2	8.50	8.40	3.88	46.37	4.89	706	57.41	17.68	10.96
Hailiutu-13	15.9	8.48	8.04	3.70	44.28	4.75	695	57.61	16.59	9.77
Hailiutu-14	14.4	8.41	8.26	3.68	44.21	5.57	801	56.96	16.86	7.94
Hailiutu-15	8.7	8.35	9.56	3.84	46.38	4.46	904	60.20	16.56	6.31
Hailiutu-16	11.7	8.50	9.37	3.70	44.33	4.81	633	59.16	17.10	9.12
Hailiutu-17	16.2	8.50	8.47	3.62	43.28	4.89	651	57.56	16.20	10.00
Groundwater										
Hailiutu-01-G	15.0	7.26	1.59	8.68	119.29	9.29	27349	80.36	46.53	1.70
Hailiutu-02-G	12.8	7.71	1.63	4.88	61.62	5.34	5304	65.99	26.45	2.29
Hailiutu-03-G	12.1	7.36	0.26	4.74	63.84	6.61	11465	57.67	13.03	0.89
Hailiutu-04-G	14.3	7.68	2.09	5.16	65.29	5.29	6117	73.69	24.88	2.63
Hailiutu-05-G	10.2	7.70	0.90	4.32	54.79	4.93	4667	60.85	17.18	1.74
Hailiutu-06-G	14.6	7.39	0.73	5.36	71.27	6.75	12454	68.75	24.36	1.35
Hailiutu-07-W	13.7	8.04	2.08	3.02	37.00	5.51	1545	46.96	12.66	2.45
Hailiutu-08-G	16.7	7.81	4.94	3.24	40.33	3.85	2927	60.02	11.92	2.14
Hailiutu-09-W	13.1	8.00	4.75	2.62	32.19	3.73	1461	36.50	12.77	1.51
Hailiutu-10-G	11.6	7.54	1.13	5.24	67.97	7.39	8320	82.99	23.21	2.00
Hailiutu-11-G	15.6	7.38	2.15	6.58	87.52	15.45	15834	95.85	27.79	2.19
Hailiutu-12-G	14.4	7.57	1.00	4.12	52.95	5.53	6304	71.96	12.20	1.70
Hailiutu-13-G	13.3	7.55	2.77	4.80	61.99	6.49	7593	96.69	27.81	2.24
Hailiutu-14-G	13.8	7.33	0.25	6.60	89.22	12.30	17446	96.37	28.07	1.86
Hailiutu-15-G	9.2	7.47	0.20	7.00	92.48	8.89	12720	128.50	29.78	2.95
Hailiutu-16-G	13.9	8.05	7.37	2.44	29.87	7.61	1223	44.54	7.91	2.00
Hailiutu-17-G	14.0	7.38	1.76	6.82	91.01	7.62	16102	108.40	31.87	2.34

Table S3. Measured values for quantifying the reach-scale CO_2 budget. The Hailiutu-07-W and Hailiutu-09-W are groundwater collected from wells, while others are the riparian groundwater.

Parameters	Values
temperature	13.43 ℃
pH	7.6
pe	4
Ca^{2+}	75.06 mg/L
Mg^{2+}	22.26 mg/L
Alkalinity	5.04 meq/L

Table S4. Initial model parameters for modeling IAP/K calcite value change after the CO_2-rich groundwater discharged to the stream.

River points	Distance	Stream		Groundwater	
		$\delta^{13}C_{DIC}$	SD	$\delta^{13}C_{DIC}$	SD
-	km	‰	‰	‰	‰
Hailiutu-01	0	-10.29	0.03	-6.15	0.09
Hailiutu-02	1.57	-9.42	0.02	-12.01	0.02
Hailiutu-03	3.37	-10.66	0.03	-12.41	0.03
Hailiutu-04	5.83	-10.52	0.04	-12.49	0.02
Hailiutu-05	7.52	-10.21	0.03	-10.91	0.05
Hailiutu-06	9.30	-10.13	0.03	-13.86	0.02
Hailiutu-07	11.05	-10.74	0.03	-11.45	0.03
Hailiutu-08	13.57	-10.70	0.05	-11.17	0.06
Hailiutu-09	15.99	-10.69	0.04	-10.01	0.06
Hailiutu-10	18.41	-10.24	0.05	-12.79	0.03
Hailiutu-11	21.29	-10.31	0.06	-13.87	0.04
Hailiutu-12	24.37	-10.49	0.07	-12.18	0.03
Hailiutu-13	27.39	-10.71	0.05	-12.47	0.03
Hailiutu-14	30.44	-10.88	0.03	-13.74	0.03
Hailiutu-15	34.08	-10.68	0.04	-12.35	0.02
Hailiutu-16	38.09	-10.76	0.03	-9.81	0.08
Hailiutu-17	42.98	-10.41	0.03	-14.56	0.03

Table S5. $\delta^{13}C_{DIC}$ values of the Hailiutu River and its adjacent groundwater. All $\delta^{13}C_{DIC}$ are reported as per mil deviation (‰) from the standard Vienna Pee Dee Belemnite (VPDB). SD represents the standard deviation. The Hailiutu-07 and Hailiutu-09 groundwater samples are groundwater collected from wells, and others are riparian groundwater.

Location	Stream type	pCO_2 (μatm)[a]	Stream CO_2 evasion (g C m^{-2} d^{-1})[a]	Reference
Scotland, UK	peatland	174-2678 (1136)	0.07-110.94 (9.33)	Long et al. (2015)
Scotland, UK	peatland	420-4500 (-)	0.26-45.88 (-)	Hope et al. (2001)
UK[b]	peatland	671-10271 (-)	0-43.2 (-)	Billett and Harvey (2013)
Connecticut, USA	forest	667-11104 (3534)	0.75-66.23 (7.40)	Aho and Raymond (2019)
Northern Sweden	forest	722-24167 (-)	3.99-17.56 (-)	Wallin et al. (2013)
Northern Sweden	forest	2015-7838 (-)	- (6.45)	Öquist et al. (2009)
Tennessee, USA	forest	360-6228 (-)	1.88-4.48 (-)	Jones and Mulholland (1998)
Northern Czech Republic	forest	450-3749 (-)	0.02-59.5 (5.90)	Marx et al. (2018)
Alps, Swiss	Alpine	309-1305 (634)	18.66-44.69 (31.20)	Horgby et al. (2019)
Northern China	Semiarid	470-1131 (719)	0.62-3.18 (1.40)	This study

Table S6. Comparison of CO_2 evasion rates from different headwater streams. [a] pCO_2 and stream CO_2 evasion rates are expressed as minimum-maximum (mean). [b] This research surveyed headwater streams in six UK peatland catchments.

Supporting references

Aho, K. S., and Raymond, P. A. (2019). Differential response of greenhouse gas evasion to storms in forested and wetland streams. *Journal of Geophysical Research: Biogeosciences*, *124*(3), 649-662.

Billett, M. F., and Harvey, F. H. (2013). Measurements of CO_2 and CH_4 evasion from UK peatland headwater streams. *Biogeochem.*, *114*(1-3), 165-181.

Clark, I. D., and Fritz, P. (1997), *Environmental Isotopes in Hydrogeology*, CRC Press, Taylor & Francis Group, New York.

Cook, P. G. (2013). Estimating groundwater discharge to rivers from river chemistry surveys. *Hydrological Processes*, *27*(25), 3694-3707.

Cook, P. G., Favreau, G., Dighton, J. C., and Tickell, S. (2003). Determining natural groundwater influx to a tropical river using radon, chlorofluorocarbons and ionic environmental tracers. *Journal of Hydrology*, *277*(1-2), 74-88.

Cook, P. G., Lamontagne, S., Berhane, D., and Clark, J. F. (2006). Quantifying groundwater discharge to Cockburn River, southeastern Australia, using dissolved gas tracers ^{222}Rn and SF_6. *Water Resources Research*, *42*(10).

Hope, D., Palmer, S. M., Billett, M. F., and Dawson, J. J. C. (2001). Carbon dioxide and methane evasion from a temperate peatland stream. *Limnology and Oceanography*, *46*(4), 847-857.

Horgby, Å., Canadell, M. B., Ulseth, A. J., Vennemann, T. W., and Battin, T. J. (2019). High-resolution spatial sampling identifies groundwater as driver of CO_2 dynamics in an Alpine stream network. *Journal of Geophysical Research: Biogeosciences*, *124*(7), 1961-1976.

Jones, J. B., and Mulholland, P. J. (1998). Carbon dioxide variation in a hardwood forest stream: An integrative measure of whole catchment soil respiration. *Ecosystems*, *1*(2), 183-196.

Long, H., Vihermaa, L., Waldron, S., Hoey, T., Quemin, S., and Newton, J. (2015). Hydraulics are a first‐order control on CO_2 efflux from fluvial systems. *Journal of Geophysical Research: Biogeosciences*, *120*(10), 1912-1922.

Ma, H., Yang, Q., Yin, L., Huang, J., Zhang, J., Wang, X., et al. (2017). Isotopic Implications for Vapor-Liquid Infiltration Pattern in the Desert Area of Ordos Plateau, China. *Clean Soil Air Water*, *45*(5).

Marx, A., Conrad, M., Aizinger, V., Prechtel, A., van Geldern, R., and Barth, J. A. C. (2018). Groundwater data improve modelling of headwater stream CO_2 outgassing with a stable DIC isotope approach. *Biogeosciences*, *15*(10), 3093-3106.

McCallum, J. L., Cook, P. G., Berhane, D., Rumpf, C., and McMahon, G. A. (2012). Quantifying groundwater flows to streams using differential flow gaugings and water chemistry. *Journal of Hydrology*, *416-417*, 118-132.

Öquist, M. G., Wallin, M., Seibert, J., Bishop, K., and Laudon, H. (2009). Dissolved Inorganic Carbon Export Across the Soil/Stream Interface and Its Fate in a Boreal Headwater Stream. *Environmental Science & Technology*, *43*(19), 7364-7369.

Plummer, L. N., and Busenberg, E. (1982). The solubilities of calcite, aragonite and vaterite in CO_2-H_2O solutions between 0 and 90°C, and an evaluation of the aqueous model for the system $CaCO_3$-CO_2-H_2O. *Geochimica et Cosmochimica Acta*, *46*(6), 1011-1040.

Raymond, P. A., Zappa, C. J., Butman, D., Bott, T. L., Potter, J., Mulholland, P., et al. (2012). Scaling the gas transfer velocity and hydraulic geometry in streams and small rivers. *Limnology and Oceanography: Fluids and Environments*, *2*(1), 41-53.

Wallin, M. B., Grabs, T., Buffam, I., Laudon, H., Ågren, A., Öquist, M. G., et al. (2013). Evasion of CO_2 from streams – The dominant component of the carbon export through the aquatic conduit in a boreal landscape. *Global Change Biology*, *19*(3), 785-797.

Xie, Y., Cook, P. G., Shanafield, M., Simmons, C. T., and Zheng, C. (2016). Uncertainty of natural tracer methods for quantifying river–aquifer interaction in a large river. *Journal of Hydrology*, *535*, 135-147.